JOURNAL OF GEOPHYSICAL RESEARCH, VOL. 86, NO. A9, PAGES 7617–7626, SEPTEMBER 1, 1981

Radar Measurements of High-Latitude Ion Composition Between 140 and 300 km Altitude

JOHN D. KELLY AND VINCENT B. WICKWAR

SRI International, Menlo Park, California 94025

The Chatanika radar has been used to measure the ratio of atomic (O^+) ions to molecular (O_2^+, NO^+) ions in the high-latitude ionosphere. The radar results agreed well with simultaneous in situ rocket data, giving confidence in the radar method of deducing ion composition. Measurements made over long periods of time show seasonal variations, diurnal variations, and variations due to auroral processes. The transition altitude, where the number densities of atomic and molecular ions are equal, is a convenient parameter for describing the composition variation with altitude or 'composition altitude profile.' The transition altitude occurs at ~190 km at night and ~170 km during the day, in agreement with midlatitude results. During the winter the daytime transition altitude is 15 km lower than in summer, a seasonal variation similar to that at midlatitudes. Energetic particle precipitation results in the lowering of the transition altitude, by 10 km in one case when energetic particles deposited ~20 ergs/cm^2 s in the atmosphere. The largest variations in ion composition were found during periods of large joule heat input resulting from electric fields on the order of 50 mV/m. The transition altitude increased by 50 km in a case where the joule heat input rate was 30 ergs/cm^2 s. These observations were compared to calculations from a simple steady state model involving the principal consituents and reactions. The results indicate that the transition altitude during particle precipitation is most influenced by the increased ion production. There do not appear to be significant effects from possible increases of N_2 vibrational temperature. A number of interrelated effects contribute to the increase in transition altitude during joule heating. The most important effect is the electric field contribution in raising the effective ion temperature. In addition, it appears that increased N_2 density is also required to account for the observed change.

1. INTRODUCTION

Theoretical studies of the high–latitude ionosphere predict that there should be large changes in ion composition as a result of energy and momentum input from the magnetosphere during auroral activity [*Schunk et al.*, 1975, 1976; *Jones and Rees*, 1973]. Rocket and satellite measurements have indeed shown that during magnetic activity the relative aboundance of light (O^+) and heavy (NO^+ and O_2^+) ions can be very different from that of the midlatitude ionosphere. One of the most striking variations was measured by the ISIS 2 satellite during the solar proton event of August 1972. During the peak of that magnetic storm, the satellite measured large concentrations of NO^+ at 1400 km, as compared to the trace amounts that are normally measured at that altitude [*Hoffman et al.*, 1974].

Incoherent scatter radars at midlatitudes have proven very useful for the study of the altitude and time variation of ion composition [*Evans*, 1967; *Evans and Cox*, 1970; *Wand and Perkins*, 1970; *Alcayde et al.*, 1974]. In this paper we adapt and extend the radar analysis techniqies of ion compositon used previously at midlatitudes, to the auroral region. As a result, using the Chatanika radar (described by *Leadabrand et al.* [1972]), we are able to make the first long-term measurements of ion composition in the auroral region. The results found in this study are consistent with both theory and previous experiments. We expect that future, more extensive studies of the composition can be used to enable us to understand the variations of the high-latitude neutral atmosphere on both short (substorm) and long (seasonal) time scales.

2. TECHNIQUE

Ground-based incoherent scatter radar is well suited for determining both temporal and spatial variations of ionospheric parameters such as the electron density, ion velocity, electron and ion temperatures, and the ion mass, all as functions of altitude. The electron density is derived from the received backscattered power, the ion drift velocity from the Doppler shift, and the electron-to-ion-temperature ratio (T_e/T_i) and the ion-temperature-to-ion-mass ratio (T_i/m_i) from the autocorrelation function (ACF) of the received signal [*Farley*, 1969; *Dougherty and Farley*, 1960; *Hagfors*, 1961; *Moorcroft*, 1964; *Waldteufel*, 1971; *Evans*, 1969].

The temperatures and composition are found by means of a least squares fitting of theoretical ACF's with the measured ACF's [*Wickwar*, 1974; *Waldteufel*, 1971]. When one examines the autocorrelation functions computed from the backscattered signals, one finds that, since the ACF functional dependences on temperature and ion composition are correlated, there are a number of temperatures that could be inferred depending on the ion composition. As a result, one of the three variables (T_e, T_i, m_i) must be independently measured or assumed before the other two can be determined. In the altitude region covered by this study, the ions considered are atomic (O^+) and molecular (NO^+ and O_2^+).

Fortunately, altitude regimes exist where the ion composition is known and unchanging, e.g., between 85 and 130 km molecular ions dominate and above much of the F region atomic oxygen ions dominate. It is in the transition region, where T_e, T_i, and m_i are all changing, that difficulties arise in the data analysis.

Midlatitude Case

In the transition region, the technique used by *Evans* [1967] for midlatitude studies requires modeling the T_i profiles. Evans made the following assumptions based on rocket and satellite data: (1) at low altitudes (<130 km) the dominant ions are molecular and at high altitudes (>250 km) the domi-

Paper number 1A0692.
0148-0227/81/001A-0692$01.00

nant ion is O^+; (2) at altitudes below ~300 km the ions are in thermal equilibrium with the neutrals.

The model used by Evans for T_i corresponds to a neutral temperature profile from Cira (1965). The particular T_n profile is chosen by using values of T_i measured at altitudes (130 and 250 km) where one can safely assume the ion composition to be entirely molecular and atomic, respectively. Composition profiles can then be determined because T_i ($T_i = T_n$) is known throughout the altitude region where the ion composition is changing from molecular to atomic. The ion composition results are, therefore, somewhat dependent on the neutral temperature model chosen.

High-Latitude Case

At high latitudes, the magnetic field lines couple the ionosphere to the magnetosphere, giving rise to energy input into the ionosphere from energetic particle precipitation and from joule heating by the convection electric field. Theory and observation [*Walker and Rees*, 1968; *Rees and Walker*, 1968] show that particle precipitation leads to an increase of the electron temperature, and joule heating leads to an increase of the ion temperature. Recent observations [*Schlegel and St. Maurice*, 1981; *Wickwar et al.*, 1981] show that coincident with joule heating, there is an increase of the *E*-region but not of the *F* region electron temperature.

The midlatitude technique for finding the ion compositon in the transition region can be applied when the ions are not heated above the neutral temperature. Therefore, the technique can still be applied to high-latitude data during periods when the effects of joule heating are small. Indeed, we have confirmed this with a comparison to a simultaneous rocket measurement of in situ ion composition (section #3). However, the midlatitude technique cannot be applied during joule heating events that are large enough to significantly increase the ion temperature above the neutral temperature. For this situation we have developed another technique. Instead of constraining T_i to fit a model T_n profile, we constrain T_e at each altitude to have a value consistent with the values measured before and after the heating event. Then the least squares fitting procedure is used to solve for T_i and m_i.

The rationale for adopting this procedure is based on the following:

1. When *F* region temperatures are deduced under the assumption of unchanging O^+ composition, a large apparent decrease in T_e is found during periods of joule heating. This apparent decrease is an artifact of the constant O^+ composition assumption. The assumption of atomic ions rather than a mixture of atomic and molecular ions results in an underestimate of both the temperature ratio, T_e/T_i, and the ion temperatures. As a result, T_e is substantially underestimated.

2. Real decreases in the electron temperature can arise from four principal sources: decrease of the solar EUV, decrease of low-energy particle precipitation, increase of the electron density, and an increase of neutral density. The first three sources can be monitored and their effects evaluated; the solar EUV through knowledge of the solar zenith angle, the soft particle flux through the particle energy deposition, and the electron density through direct measurement. In fact, the effects of the second and third sources are in opposite directions. For example, a decrease in soft particle flux will decrease the thermal energy input and also have the effect of reducing the electron density, which, in turn, leads to a reduction in the electron-neutral loss rate. As a result, the change in T_e is small. Although an increase in neutral density will increase the loss rate, in the cases we observed, neutral density increases were modest and did not compensate for the terms that would cause heating. Constraining T_e to vary slowly and smoothly between its preheating and postheating event values accounts to first order for these possible real sources of T_e decrease.

In fact, one would expect joule heating to result in increased electron temperature in most cases and thus our analysis technique results in a lower bound in both electron and ion temperatures and the percentage of molecular ions. To evaluate the effects of joule heating on T_e, calculations were performed under a number of different conditions using the energy loss and input rates from *Schunk and Nagy* [1978], *Stubbe and Varnum* [1972], *Prasad and Furman* [1973], and *Hoegy* [1976], and assumed that the external energy sources—low energy particle precipitation or solar EUV—were constant.

The changes during periods of joule heating that would increase the electron temperature are: decreased electron density, increased ion temperature, and conversion of atomic ions to molecular ions. A decrease of electron density by up to a factor of 2 is often observed. This has a significant effect because it reduces all electron-neutral loss rates by this amount, tending to increase T_e. An increase in the ion temperature of 300 to 1000 K will greatly reduce the energy loss from electrons to ions and will often lead to energy input to the electrons from hotter ions. This effect is much more important at the higher altitudes and for the higher electron densities. Finally, the conversion of atomic to molecular ions is comparatively unimportant.

The joule heating-induced change that would decrease the electron temperature is increased neutral density. The effect of an increase in neutral density is considered because it has often been reported in connection with the auroral region [e.g., *Prölss*, 1980]. Even a fourfold increase in the N_2 density would not decrease the electron temperature sufficiently to fully compensate for the temperature increase sources considered above. Increases in the O_2 density would further increase the electron-neutral losses, but are much less important. Increases in the O density would be important, but have not been observed. Thus, in general, the electron temperature should, in theory, increase during joule heating and our assumption of a constant T_e does provide a lower bound for the proportion of molecular ions and for the transition altitude.

The procedures we follow to determine the ion compositon at high latitudes and the choice between procedures are summarized in the flowchart in Figure 1.

3. OBSERVATIONS

The measurements were made with the Chatanika radar [*Leadabrand et al.*, 1972] that is located near Fairbanks, Alaska, at 65°N geographic and geomagnetic latitude. The autocorrelation function measurements were made using both a 320-μs and a 160-μs transmitted pulse at 1290 MHz together with hardware correlators. The system is described and references given in *Kofman and Wickwar* [1980]. The antenna was cycled between three positions or kept scanning in azimuth during the observations so as to determine the vector ion velocities (electric fields) and the joule heating rate [*Brekke and Rino*, 1978] in addition to T_e, T_i, and ion composition.

The ion composition varies from a mixture of NO^+ and O_2^+

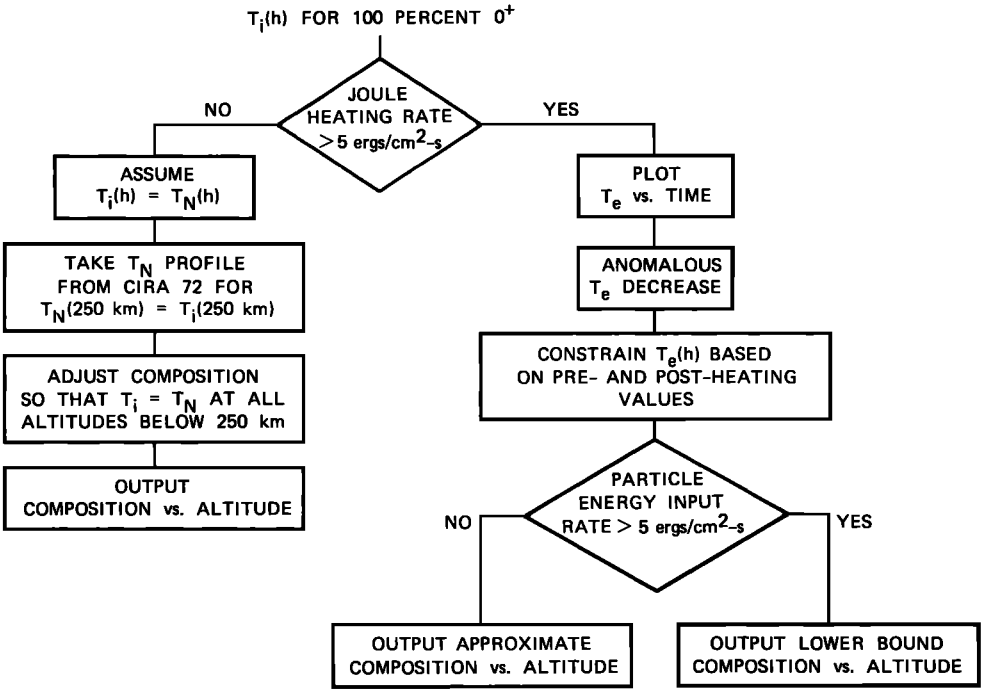

Fig. 1. Technique for the determination of ion composition profiles.

in the lower E region to O^+ in the upper F region. We usually describe it in terms of the fraction that is made up of atomic ions. In addition, a single parameter that succinctly describes the composition is the transition altitude, the altitude where the ion composition is half atomic and half molecular. The variation of this parameter with time, season, and auroral activity (both particle precipitation and joule heating) was studied.

The transmitted pulses, particularly the 320-μs pulse, are longer than optimum at the low-altitude end of the altitude scale, although they do have the distinct advantage of yielding good signal-to-noise ratios. There is, however, the possibility of small, systematic errors in the altitude because the temperature averaged over the sampled region may not be the temperature at the midpoint of the pulse. The difference depends on the gradients of the measured parameters (T_e, T_i, and composition), the weighting effect of the electron density gradient, the pulse length, and the details of the measurement technique. Using gradients measured during day and night conditions, this source of error was evaluated and the resulting bias in the transition altitude calculation was found to be less than 5 km. We consider this acceptable because the geophysical effects that we are observing vary the transition altitude by 20 to 50 km.

A set of three 24-hour periods supplemented by one shorter period were chosen to study the variation of composition with time, season, and auroral activity. The days examined are given in Table 1 with local magnetic activity indices and the solar zenith angle extremes.

Comparison With In Situ Ion Composition Measurements

On February 28, 1976, a Nike Tomahawk rocket carrying a University of Texas at Dallas (UTD) payload was launched from Poker Flat, Alaska, 3 km from the Chatanika radar. The payload instrumentation included probes for measuring ion and electron densities and a positive ion mass spectrometer. The densities were measured on the upleg and the ion composition on the downleg.

The radar was operated before, during, and after the flight in order to obtain background as well as simultaneous data. The antenna was operated in the three-position mode described earlier and the pulse length used was 160 μs, allowing a 24-km range resolution. The background data include both joule and particle energy input rates, shown in Figure 2. During the rocket flight, the joule heat input rate (3 ergs/cm^2 s) was relatively small, causing an enhancement in T_i of less than 100 K. Hence, the $T_i = T_n$ method was used to compute composition.

The radar beam was pointed along the rocket upleg trajectory from 1216 to 1219 UT. The electron density profile measured during that period agreed well with the profile measured by the rocket. The ion temperature data were averaged over those four minutes and an exospheric temperature of 900 K was computed. The radar data were analyzed for composition using two T_n profiles, one from Cira (1972) and one from *Banks and Kockarts* [1973]. The composition profiles and the one measured by the rocket on the downleg are shown in Figure 3. Because of the similar density profiles observed by the radar at three azimuths and the uniform postsubstorm glow in the all-sky-camera photographs, we believe that the auroral conditions were sufficiently homogeneous to allow us to compare the radar and rocket ion compositions.

Good agreement is evident between the ion composition profiles measured by the rocket and radar techniques (Figure 3). Although the agreement is better when Cira (1972) is used instead of Banks and Kockarts for the radar analysis, the results are not particularly sensitive to the assumed neutral model. The maximum differences occur below the 185-km transition altitude where the two model temperature profiles differ the most. The systematic difference in the transition alti-

TABLE 1. Solar Zenith Angle Extremes, College, Alaska, Magnetic Activity Indices, and Solar Flux Indices for Composition Study Data

UT Date	Min. SZA	Max. SZA	College, Alaska, K Index 00–03	03–06	06–09	09–12	12–15	15–18	18–21	21–24	Σ	S_{107}
Aug. 13, 1975	50	100	1	1	2	4	3	2	0	1	14	95.5
Oct. 15, 1975	74	123	1	1	1	2	2	1	1	1	10	80.8
Feb. 28, 1976					3	5	3					69.2
May 13, 1976	47	96	1	1	1	1	1	1	1	1	8	72.1

tude due to the choice of neutral model is less than 10 km for this determination, with the Cira (1972) model giving the lower altitude. For the remainder of the study, the Cira (1972) neutral model is used.

Quiet Periods

The diurnal variations in the transition altitude were examined during quiet periods of October 15 and May 13. The percentage of atomic ions was evaluated at altitudes corresponding to the midpoint of each range gate and a composition profile was constructed by fitting a curve through those data points. For the October data the radar pulse length was 320 μs, providing a 48-km range resolution. Analysis was not attempted at altitudes below about 160 km because the pulse length was large relative to the scale height. For the May data the pulse length was 160 μs. These data were analyzed down to 140 km altitude.

The October day shown in Figure 4 contained the most pronounced diurnal variation in transition altitude. This is expected since the solar zenith angle in October varies between 74° and 123°—i.e., from a sunlit to a nighttime situation. The transition altitude was a maximum during the night—approximately 190 to 200 km—and a minimum during the day—approximately 175 km at 1400 local time (0000 UT).

During the May experiment, the energy deposition and joule heat input rates were minimal. There was very little variation in the transition altitude (Figure 5). The altitude was consistently between 190 and 200 km. Pronounced diurnal variation is not expected because the solar zenith angle never exceeded 96° on that day.

Seasonal variations were examined by comparing data in May and October with the same solar zenith angles. For a solar zenith angle of 76° the transition altitude in May was about 195 km—while in October (at 1300 local) it was about 175 km. This difference, 20 km, is the maximum observed. For larger solar zenith angles in October, the transition altitude increases and approaches the relatively constant May value. This observed variation is consistent with the seasonal variation observed at midlatitudes [*Evans and Cox,* 1970; *Oliver,* 1975] and with the seasonal variation in the $[O]/[N_2]$ ratio [*Roble,* 1977] that will be discussed in a later section.

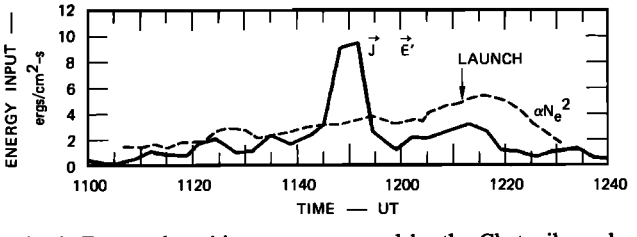

Fig. 2. Energy deposition rates measured by the Chatanika radar during rocket flight on February 28, 1976. The rocket collected data from 1219 to 1221 UT when the joule heat input rate was negligible.

Active Periods

Particle precipitation. We have examined the effect of particle precipitation on the transition altitude. A typical event took place in the early portion of the October data already presented. Between about 1100 and 1200 UT, moderate particle precipitation occurred. The particle energy input rate varied from 5 to 20 ergs/cm² s, as shown in Figure 6. During this time, the electric fields (and the joule heat input) were minimal (<3 ergs/cm² s), and consequently $T_i = T_n$ was assumed. We have already examined the transition altitude for October during the quiet period and we have found that the transition altitude during the night was ~190 km or greater. During the particle precipitation event, however, it can be seen from Figure 4 that the transition altitude decreased to ~180 km. At the peak of the event the composition profiles are quite similar to daytime profiles previously discussed.

Joule heating. The largest variation in ion composition was observed when the joule heating rate was large. Such was the case on August 13, 1975, at about 1400 UT. The temperatures, electric fields, and the joule heat input rates were computed for the full 24-hour period. As can be seen in Figure 7, the joule heating was large at 1400 UT and moderate at 1200 UT.

The electron and ion temperatures (computed with the assumption of 100 percent O^+ ions) at 277 km altitude are shown in Figure 8. Early in the experiment, 0000 to 0600 UT, the ion temperature is fairly constant with a value of 900 K. The electron temperature shows the effect of the changing solar zenith angle. Initially, during sunlit conditions, the temperature is about 2200 K and it gradually decreases with increasing solar zenith angle (from 0430 to 0800 UT). At 0900 UT, the temperature is at a minimum of about 1400 K and gradually increases again as the solar zenith angle decreases.

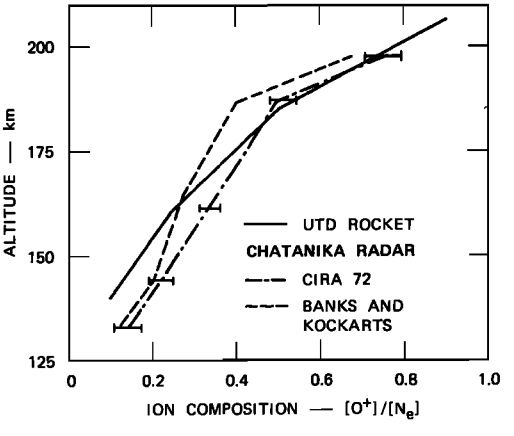

Fig. 3. Comparison of ion composition profiles from rocket and radar data. The radar-determined profiles were computed using two neutral models for an exospheric temperature of 900 K.

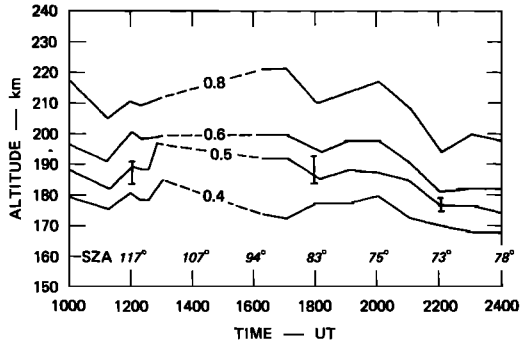

Fig. 4. Ion composition contours for October 15, 1975. The transition altitude lowers as the solar zenith angle decreases. The decrease between 1000 and 1200 UT is due to particle precipitation.

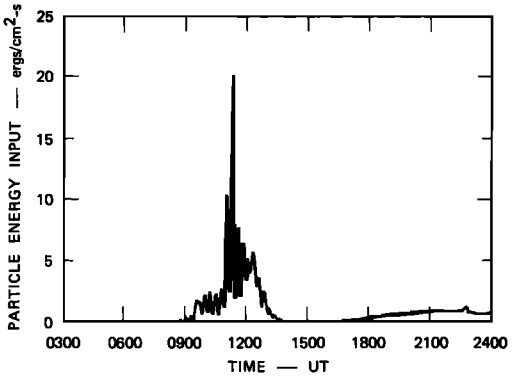

Fig. 6. Particle energy input rate for October 15, 1975.

There is little change in the ion temperature until about 1000 UT, when the joule heat input begins. There are obvious enhancements in ion temperature at 1000, 1200, and 1400 UT. The electron temperature around 1400 UT appears to decrease suggesting that the 100 percent O^+ assumption is no longer valid. The apparent dip in T_e for three altitudes is shown in Figure 9. The dip at 277 km is larger than at 218 km because of a larger relative change from atomic to molecular ions. While the dip is small at 335 km, it does indicate the presence of a significant percentage (20%) of molecular ions during the joule heating event. During this period (1330–1430 UT) the method of constraining T_e was used to compute the ion composition.

The composition contours are indicated in Figure 10. The transition altitude is seen to be near 190 km at the beginning of the observations. However, at the peak of joule heating, 1400 UT, this altitude increased by 50 km—molecular ions are predominant up to 240 km.

During this heating period, the electron density was also seen to decrease. The maximum F region electron density 30 min prior to the depletion was about $2 \times 10^5/cm^3$. During the heating, the density dropped to $10^5/cm^3$, and 30 min later it had recovered to $1.8 \times 10^5/cm^3$. In addition to transport effects, a change in the dominant F region ion from atomic to molecular should cause a decay in the electron density since molecular ions, O_2^+ and NO^+, recombine much more rapidly. Electron density profiles measured before, during, and after the heating event are shown in Figure 11.

The E region electron density was also seen to decrease during the period when the electric field was large. This decrease must be due to a reduction, or softening, of the particle precipitation and not due to a change in ion composition. At E region altitudes, the predominant ions are molecular regardless of the auroral activity.

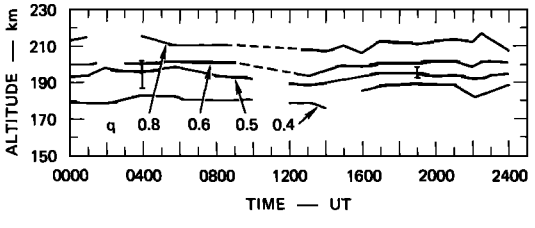

Fig. 5. Ion composition contours for May 13, 1976.

4. Discussion

To better understand the ion composition variations deduced from our data, model calculations were performed using the measured physical parameters (N_e and temperature) and the neutral model atmosphere parameters. The factors that cause variations in the ion composition can be examined with a simple numerical model involving the major constituents, the most important reactions, and their associated reaction rates:

$$O^+ + O_2 \xrightarrow{\gamma_1} O_2^+ + O \tag{1a}$$

$$O_2^+ + e \xrightarrow{\alpha_1} O + O \tag{1b}$$

$$O^+ + N_2 \xrightarrow{\gamma_2} NO^+ + N \tag{1c}$$

$$NO^+ + e \xrightarrow{\alpha_2} N + O \tag{1d}$$

$$N_2^+ + O \xrightarrow{\gamma_3} NO^+ + N \tag{1e}$$

$$N_2^+ + e \xrightarrow{\alpha_3} N + N \tag{1f}$$

where

$$\gamma_1 = 2 \times 10^{-11} \left(\frac{300}{T_i}\right)^{1/2} \text{cm}^3/\text{s} \tag{2a}$$

$$\alpha_1 = 2.2 \times 10^{-7} \left(\frac{300}{T_e}\right) \text{cm}^3/\text{s} \tag{2b}$$

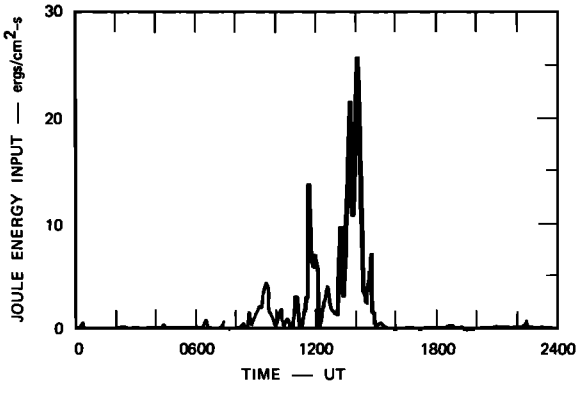

Fig. 7. Joule heat input rate on August 13, 1975.

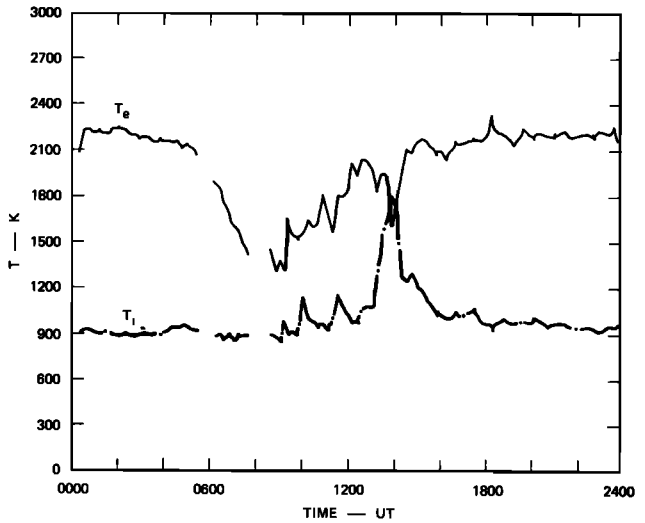

Fig. 8. Electron and ion temperatures computed for 100% O^+ at 277 km altitude on August 13, 1975. A diurnal variation in T_e can be seen. During the period of joule heating (1400 UT) the ion temperature is enhanced coincident with an anomalous decrease in electron temperature indicating a change in the ion composition.

$$\gamma_2 = 1 \times 10^{-12}\left(\frac{300}{T_i}\right) \text{cm}^3/\text{s} \tag{2c}$$

$$\alpha_2 = 4.1 \times 10^{-7}\left(\frac{298}{T_e}\right) \text{cm}^3/\text{s} \tag{2d}$$

$$\gamma_3 = 1.4 \times 10^{-10}\ \text{cm}^3/\text{s} \tag{2e}$$

$$\alpha_3 = 2.9 \times 10^{-7}\left(\frac{300}{T_e}\right)^{1/3} \text{cm}^3/\text{s} \tag{2f}$$

The reaction rate coefficients are taken from *Jones and Rees* [1973].

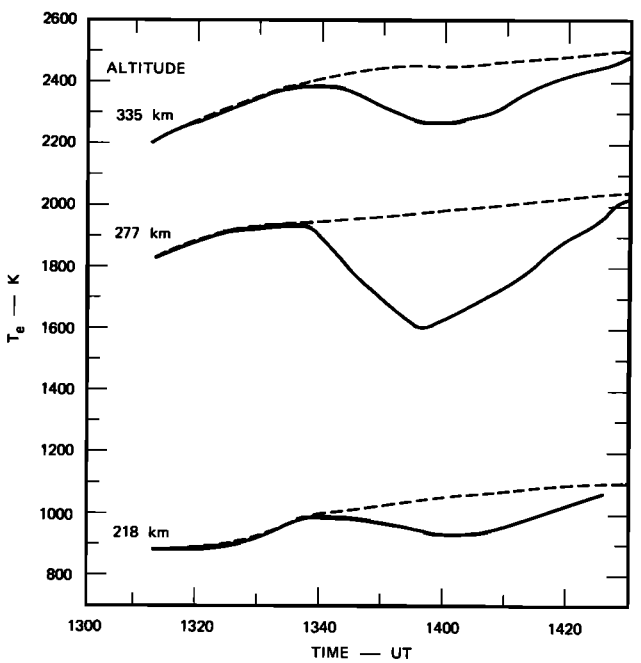

Fig. 9. Electron temperatures computed at three altitudes for 100% O^+ Around 1400 UT on August 13, 1975.

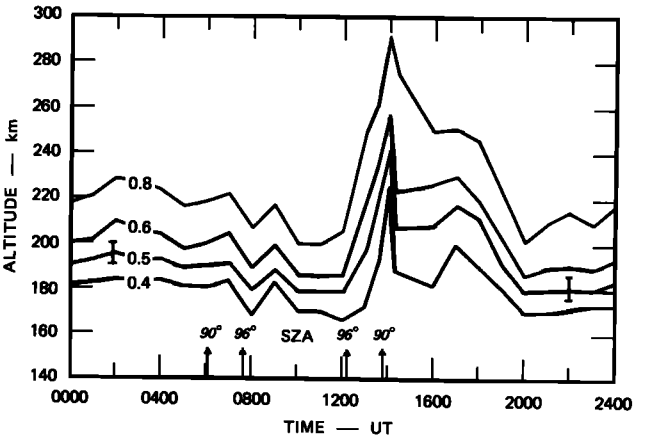

Fig. 10. Ion composition contours for August 13, 1975.

The continuity equation for each species is expressed as

$$\frac{\partial[X^+]}{\partial t} = q(X^+) - L \tag{3}$$

where $[X^+]$ is the number density of species X^+, $q(X^+)$ is the production rate of species X^+, and L is the loss rate, when dynamical factors are unimportant, as we will assume for this analysis. For steady state conditions and charge neutrality ($N_e = [O^+] + [NO^+] + [O_2^+]$), the continuity equations can be combined and solved for the fraction of atomic ions

$$\frac{[O^+]}{N_e} = \left\{1 + \frac{\gamma_1[O_2]}{\alpha_1 N_e} + \frac{\gamma_2[N_2]}{\alpha_2 N_e} + \left[\frac{\gamma_1[O_2] + \gamma_2[N_2]}{q(O^+)}\right]\left[\frac{\gamma_3[N_2^+][O]}{\alpha_2 N_e} + \frac{q[O_2^+]}{\alpha_1 N_e}\right]\right\}^{-1} \tag{4}$$

where

$$q(O^+) = \frac{0.56[O]\eta}{1.15[N_2] + 1.5[O_2] + 0.56[O]} \tag{5a}$$

$$q(O_2^+) = \frac{[O_2]\eta}{1.15[N_2] + 1.5[O_2] + 0.56[O]} \tag{5b}$$

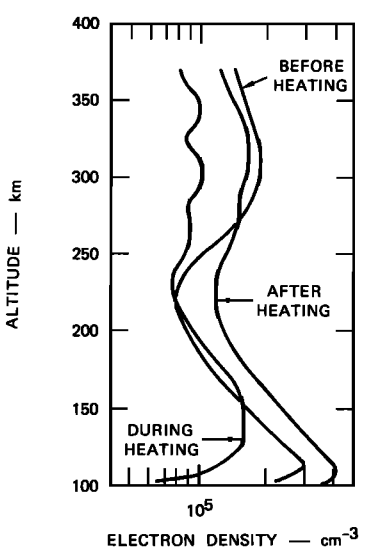

Fig. 11. Electron density profiles for period of joule heating on August 13, 1975.

TABLE 2. Ionospheric Data and Model Atmosphere for Quiet Day and Quiet Night Comparison

	Quiet Day						Quiet Night		
Altitude, km	N_e, cm^{-3}	T_i, K	T_e, K	$[O_2]$, cm^{-3}	$[O]$, cm^{-3}	$[N_2]$, cm^{-3}	N_e, cm^{-3}	T_i, K	T_e, K
140	7.5E4	596	650	6.22E9	3.78E10	5.37E10	8.6E4	596	596
160	1.0E5	765	1000	1.55E9	1.66E10	1.54E10	7.0E4	765	765
180	1.2E5	861	1600	5.26E8	9.10E9	5.89E9	5.6E4	861	861
200	1.5E5	916	1800	2.07E8	5.51E9	2.59E9	5.0E4	916	916
220	2.0E5	948	2000	8.87E7	3.52E9	1.22E9	3.4E4	948	948
240	3.0E5	967	2000	3.99E7	2.33E9	6.04E8	3.0E4	967	967
260	2.5E5	979	2000	1.86E7	1.57E9	3.09E8	2.8E4	979	979
280	2.45E5	986	2000	8.85E6	1.07E9	1.61E8	2.6E4	986	986
300	2.0E5	991	2000	4.30E6	7.45E8	8.55E7	2.4E4	991	991

The ionospheric data are from February 18, 1976. The neutral data are from the Cira (1972) model for an exospheric temperature of 1000 K.

$$q(N_2^+) = \frac{0.92[N_2]\eta}{1.15[N_2] + 1.50[O_2] + 0.56[O]} \quad (5c)$$

$$[N_2^+] = \frac{q(N_2^+)}{\gamma_3[O] + \alpha_3 N_e} \quad (6)$$

and η is the total ion production rate. These production rates are from *Jones and Rees* [1973].

Using (4) for the ion composition, the effects on the transition altitude of varying the atmospheric density, electron density, production rates, and temperatures can be assessed.

Diurnal Variation

Our observations indicate that at night the transition altitude increases. In the absence of auroral activity, the ionospheric parameters most affected by a change in solar zenith angle from day to night are the electron density and electron temperature. The expected diurnal variation in ion composition can be calculated by solving (4) using measured ionospheric data for N_e, T_e, T_i, and a model atmosphere for $[N_2]$, $[O_2]$, and $[O]$ (Cira, 1972). The values used are given in Table 2. The total ion production rate was adjusted during the daytime to fit the observed electron density profiles. The production rate was decreased to match measured nighttime profiles. The resultant ion composition profiles are shown in Figure 12. The difference in the profiles is most pronounced above the transition altitude where the percentage change in electron densities is greatest. In the model calculations, the transition altitude increases by 20 km at night, which is consistent with the measurements shown in section 3.

Seasonal Variation

A number of factors could be responsible for the observed seasonal variation in the transition altitude (as much as 20 km higher in May than in October): variations in the solar EUV flux and variations in the neutral atmospheric density (specifically the $[O]/[N_2]$ ratio). As shown in Table 1, there is very little change in the solar radiation as represented by the $S_{10.7}$ parameter (<10%). However, an examination of the peak electron density in the F region shows that the October day had more than twice as much ionization present. This is consistent with expected seasonal variations in the $[O]/[N_2]$, this ratio being smaller in summer than in winter [*Roble,* 1977]. Enhancing the $[N_2]$ at a given altitude relative to $[O]$ increases the O^+ loss rate, thereby decreasing the electron density and increasing the transition altitude. The model calculations indicate a small increase in transition altitude. The model calculations indicate a small increase in transition altitude (~5 km) when the $[O]$ to $[N_2]$ ratio is decreased by small amounts above 160 km to a factor of 2 at 300 km (approximated by using model values for a higher exospheric temperature). A larger N_2 variation would be needed to match the observed variation in the transition altitude.

Particle Precipitation

During enhanced particle precipitation we observe a lowering of the transition altitude. The variation can be similar in magnitude and sense to the 20-km decrease in going from night to day.

In the F_1 region, whether the ionizing source is solar EUV or auroral particle precipitation, the effects are similar. As the source strength increases, both molecular and atomic ions are created and the electron density increases. Because the O^+

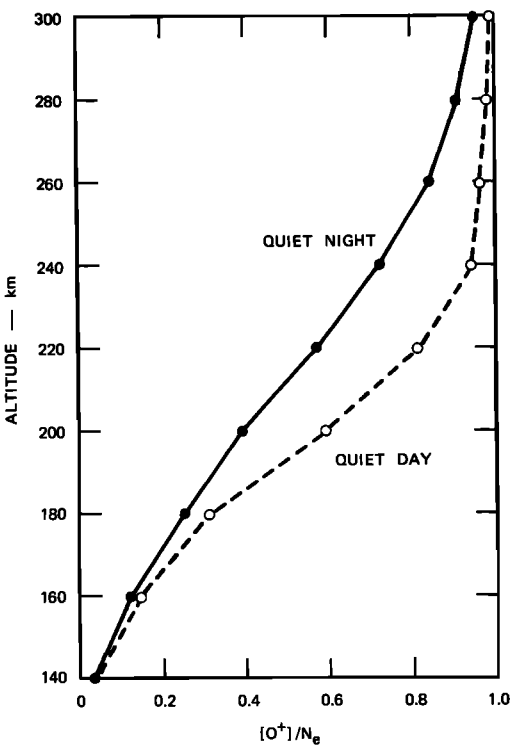

Fig. 12. Model composition profiles showing diurnal variation. The greatest difference is above the transition altitude where the percentage change in electron density is largest.

TABLE 3. Ionospheric Data for Particle Precipitation Event

Altitude, km	N_e, cm^{-3}	T_i, K	T_e, K
140	2.0E5	596	750
160	1.3E5	765	1120
180	1.5E5	861	1300
200	1.8E5	916	1800
220	1.9E5	948	2000
240	2.0E5	967	2000
260	1.9E5	979	2000
280	1.6E5	986	2000
300	1.4E5	991	2000

The data are from February 18, 1976.

lifetime is long compared to that of NO^+, O^+ dominates to lower altitudes and the transition altitude lowers.

Another point relative to the production of NO^+ is the increase in the reaction rate for $O^+ + N_2 \rightarrow NO^+ + N$, when N_2 becomes vibrationally excited [*Schunk and Banks,* 1975; *Newton et al.,* 1977] During auroral activity N_2 could become vibrationally excited N_2^* through the process [*Schunk and Banks,* 1975]

$$\begin{aligned} e + N_2 &\rightarrow N_2^* + e \\ N + NO &\rightarrow N^*_2 + O \\ O(^1D) + N_2 &\rightarrow N_2^* + O(^3P) \end{aligned} \quad (7)$$

where e is an energetic electron. The effect would be to increase the number density of NO^+ relative to O^+, thereby raising the transition altitude.

Apparently, the increase in ionization rate is more important because in the cases that we have observed (e.g., October 15, 1975), there has always been a decrease in the transition altitude.

The model calculations show a similar decrease of the transition altitude. The effects of electron precipitation considered are enhancements of electron density, electron temperature, and N_2 vibrational temperature. The ionospheric parameters are given in Table 3. The temperature and electron density profiles used are from data taken on February 18, 1976, and the reaction rate coefficient for $N_2 + O^+$ was enhanced to account for an N_2 vibrational temperature of 1400 K. The particle energy input was approximately 20 ergs/cm^2 s. The model composition profiles shown in Figure 13 indicate that relative to the background profile (quiet night) the transition altitude is lower by 25 km, in agreement with the data. This indicates that the effects of enhanced N_2 vibrational temperature are less important than the increase in ion production rate in altering the transition altitude.

Joule Heating

The measurements indicate that during periods of large joule heating the transition altitude increases substantially. As a result of this change in ion composition, the *F* region ionization rapidly decays because of enhanced recombination of the molecular ions as compared to O^+.

The observed behavior is expected both from theoretical arguments and satellite measurements. The following processes contribute to increasing the NO^+ abundance [*Banks et al.,* 1974; *Schunk et al.,* 1975, 1976; *Schunk and Banks,* 1975]: (1) enhanced $[N_2]$, (2) enhanced ion temperatures, (3) relative motion of the ions and neutrals.

Enhanced $[N_2]$ has been observed by satellites in the auroral region [e.g., *Prölss,* 1980]. It is expected to occur because, during periods of large joule heating, the neutral atmosphere should be heated by the ion-neutral collisions. A heated volume element of neutral particles will rise with a vertical velocity that increases with altitude [*Hays et al.,* 1973]. This expansion will cause an upwelling of N_2 molecules, thereby increasing the number density of N_2 at higher altitudes. The number density of NO^+ will be enhanced because more N_2 is available to either react with O^+ to form NO^+, or be ionized to form N_2^+, which in turn reacts with O to form NO^+.

The second and third factors contributing to the enhancement of NO^+ ions during heating events are the dependence of the reaction rate γ_2 for $O^+ + N_2 \rightarrow NO^+ + N$ on ion temperature, and relative motion. From *Banks et al.* [1974]:

$$\gamma_2 = 1.2 \times 10^{-12} \left(\frac{300\ \text{K}}{T_{\text{eff}}} \right) \text{cm}^3/\text{s} \quad T_{\text{eff}} < 750 \quad (8a)$$

$$\gamma_2 = 8.0 \times 10^{-14} \left(\frac{T_{\text{eff}}}{300\ \text{K}} \right)^2 \text{cm}^3/\text{s} \quad T_{\text{eff}} > 750 \quad (8b)$$

where $T_{\text{eff}} = T_i + 0.329\ \vec{E}_\perp{}'^2$, and $\vec{E}_\perp{}'^2$ is the orthogonal $\vec{E}$ field (mV/m) measured in the neutral-wind frame. This is a simplified form assuming $\nu_i/\Omega_i \ll 1$ and $B = 0.5$ gauss (polar region). As an example, for an $\vec{E}$ field of 50 m V/m, and $T_n = 900$ K, T_{eff} will be increased by a factor of 1.9, as compared to T_{eff} for no $\vec{E}$ field. This in turn increases γ_2 by a factor of 3.7. The result is an enhancement in the loss rate of atomic ions and production rate of NO^+ and, hence, an enhancement in the ratio of molecular to atomic ions. Furthermore, if for any reason there were an increase in the electron temperature, then the reaction rate α_2 for dissociative recombination of NO^+ would decrease [*Walls and Dunn,* 1974]. The net result would be an even larger increase in molecular ions relative to

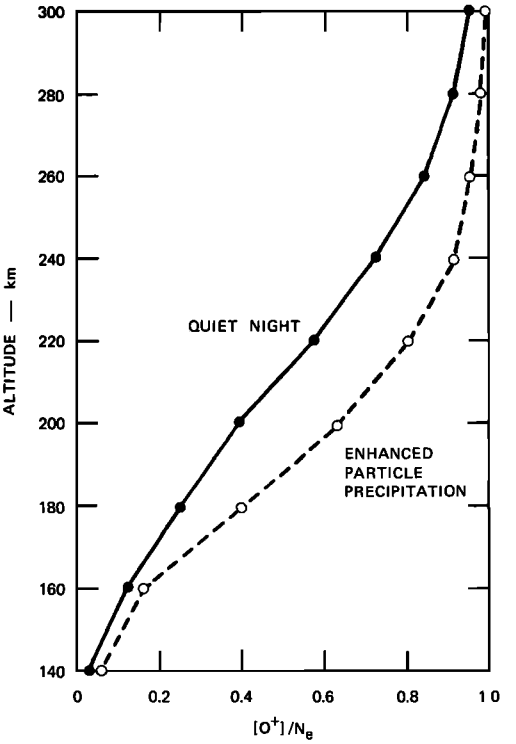

Fig. 13. Model composition profiles showing the effects of auroral ionization. The transition altitude decreased with increasing production rate.

atomic ions and, indeed, an increase in the number density of molecular ions.

The atmospheric model and ionospheric data used to numerically model the effect of joule heating are given in Table 4. The ionospheric data are from August 13, 1975. The total ion production rates were adjusted to have the ion composition match the observation prior to the joule heating event. These rates were kept constant through the joule heating period. Due to the enhanced electric field and elevated ion temperatures observed during the event, γ_2 was considerably increased. The resultant model ion composition profile (Figure 14) indicates that more molecular ions should exist at all altitudes as compared to the quiet period. However, the transition altitude is only increased by 20 km. If we further increase the N_2 density by a factor of two at 160 km (corresponding to an increase in neutral temperature of ~250°), the transition altitude is increased by a total of 40 km, in better agreement with the observation.

5. Summary and Conclusions

We have described the incoherent scatter radar techniques by which variations of ion composition in the high-latitude ionosphere can be determined. The midlatitude technique based on the equality of ion and neutral temperatures between 130 and 300 km [*Evans*, 1967] can be applied under quiet conditions, under conditions of energetic particle precipitation, and under conditions of joule heating when the heating rate is low—less than 5 ergs/cm² s. Confidence in the applicability of this technique has been gained by a comparison of radar-derived ion composition and simultaneous in situ rocket measurements of ion composition. We have developed another technique for conditions with considerable joule heating. It is based on the realistic assumption that during such periods the electron temperature will not decrease. If we assume the electron temperature is constant, we can determine a lower bound to the fraction of ionization that is due to molecular ions (NO^+ and O_2^+) rather than atomic ions (O^+).

The existence of a ground-based radar technique enables us to examine the long-term behavior of the desired parameter, ion composition. In addition, the other parameters that can be determined from the radar measurements can be used to understand the variations in the ion composition. For simplicity of discussion we examine in detail only the time variation of the transition altitude, the altitude at which the composition is half molecular ions and half atomic. During the winter when there is a definite day and a definite night, the transition altitude increased from 175 km during the day to 190 km at night. In the summer, when the sun never sets on the ionosphere, the transition altitude remained consistently near 190 km. These two quiet time situations are very similar to the diurnal variation and the daytime winter-summer variation observed at midlatitude. During winter-nighttime particle precipitation events, the transition altitude decreases on the order of 10 to 20 km, depending on the energy input. The most dramatic changes occur during joule heating events when the transition altitude increases sharply—e.g., 50 km for one 30 erg/cm² s event.

TABLE 4. Ionospheric Data and Model Atmosphere for Period of Joule Heating

Altitude, km	N_e, cm^{-3}	T_i, K	T_e, K	$[O_2]$, cm^{-3}	$[O]$, cm^{-3}	$[N_2]$, cm^{-3}
140	7.5E4	1590	600	6.22E9	3.78E10	5.37E10
160	1.0E5	1780	780	1.55E9	1.66E10	1.54E10
180	1.2E5	1910	1050	5.26E8	9.10E9	5.89E9
200	1.0E5	2000	1300	2.07E8	5.51E9	2.59E9
220	9.0E4	2050	1550	8.87E7	3.52E9	1.22E9
240	9.2E4	2100	1750	3.99E7	2.33E9	6.04E8
260	1.0E5	2130	1900	1.86E7	1.57E9	3.09E8
280	1.2E5	2150	2050	8.85E6	1.07E9	1.61E8
300	1.2E5	2200	2250	4.30E6	7.45E8	8.55E7

The ionospheric data come from August 13, 1975.

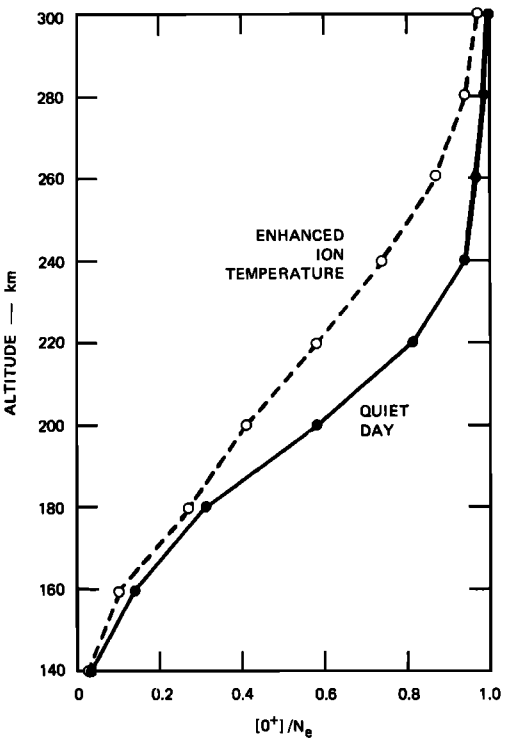

Fig. 14. Model composition profiles showing the effect of joule heat input. The transition altitude increased as the ion temperature was enhanced.

We compared our data with a simple steady state model of the ion chemistry using the important reactions to examine these variations in the ion composition. The observed diurnal and seasonal variations are similar to those seen at midlatitudes and are presumably due to the same causes. Indeed, the simple model calculations do show that the diurnal variation can be accounted for by the changes in photoionization with varying solar zenith angles, and that the seasonal variation is consistent with an increasing [O] to [N_2] ratio from summer to winter.

During periods of particle precipitation three things are expected to happen: ion production rates increase, electron temperatures increase, and N_2 becomes vibrationally excited. The first would cause the transition altitude to decrease; the other two would cause it to increase. The modeling shows that the effect in transition altitude of an increased ion production rate is much more important than the effect of an increased electron temperature. The fact that we observe a decrease in the transition altitude shows that the increased ion production rate is also more important than vibrational excitation of N_2. For this to be the case, the modeling shows that either the vibrational temperature has to be low or the vibrationally enhanced reaction rates are in error. Increased N_2 density appears to be unimportant.

During periods of substantial joule heating there are again three things that we expect: N_2 density increase, ion temperature enhancement, and large relative ion-neutral velocities. All three would lead to increases in the transition altitude by increasing the rate of conversion of O^+ to NO^+. For the case examined here the modeling shows that the relative ion-neutral velocity can account for 40% of the change in the transition altitude. The change in ion temperature has a smaller effect. This implies that there must be an increase in the N_2 density—e.g., a factor of 2.5 at 277 km—to help account for the change in transition altitude. The importance of an N_2 density increase for the ion composition variation during joule heating is very different from the particle precipitation situation.

Thus, for the first time we have examined the ion composition in the auroral region using incoherent scatter. Under quiet conditions, the behavior is similar to that observed at midlatitudes. Under active conditions, both particle precipitation and joule heating produce significant changes in ion composition. By comparison of observation and model, we have shown that for particle precipitation the most important factor contributing to a decrease in transition altitude is an enhanced ion production rate. For joule heating, the two important factors contributing to an increase in transition altitude are a large differential ion-neutral velocity and an increase in the N_2 density.

Acknowledgments. We would like to thank A. B. Christensen, formerly of the University of Texas at Dallas, now of Aerospace Corporation, for permission to use the rocket data prior to publication. We would also like to thank M. H. Rees of the Geophysical Institute, University of Alaska, for numerous valuable discussions. We would finally like to thank numerous members of the staff of the Radio Physics Laboratory, SRI International, who are involved in the operation of the Chatanika radar and the reduction of the data. In particular, we would like to acknowledge the invaluable assistance of Mary McCready in all phases of the data reduction and analysis. This research was carried out under contract DNA001-77-C-0042 from the Defense Nuclear Agency and several grants from the Division of Atmospheric Sciences, National Science Foundation. The Chatanika radar is operated by SRI International under a grant from the Aeronomy Program, National Science Foundation.

The Editor thanks R. H. Wand for his assistance in evaluating this paper.

REFERENCES

Alcayde, D., P. Bauer, and J. Fontanari, Long-term variations of thermospheric temperature and composition, *J. Geophys. Res., 79,* 629–637, 1974.

Banks, P. M., and G. Kockarts, *Aeronomy,* pp. 329–338, Academic, New York, 1973.

Banks, P. M., R. W. Schunk, and W. J. Raitt, NO^+ and O^+ in the high-latitude *F*-region, *Geophys. Res. Lett., 1,* 239–242, 1974.

Brekke, A., and C. L. Rino, High-resolution altitude profiles of the auroral zone energy dissipation due to ionospheric currents, *J. Geophys. Res., 83,* 2517–2524, 1978.

Dougherty, J. P., and D. T. Farley, A theory of incoherent scattering of radio waves by a plasma, *Proc. R. Soc. A, 259,* 79–99, 1960.

Evans, J. V., Midlatitude *F*-region densities and temperatures at sunspot minimum, *Planet. Space Sci., 15,* 1387–1405, 1967.

Evans, J. V., Theory and practice of ionosphere study by Thomson scatter radar, *Proc. IEEE, 57,* 496–530, 1969.

Evans, J. V., and L. P. Cox, Seasonal variation of the F_1 region ion composition, *J. Geophys. Res., 75,* 159–164, 1970.

Farley, D. T., Incoherent scatter correlation function measurement, *Radio Sci., 4,* 143, 1969.

Feder, J. A., and P. M. Banks, Convection electric fields and polar thermospheric winds, *J. Geophys. Res., 77,* 2328–2340, 1972.

Hagfors, T., Density fluctuations in a plasma in a magnetic field with applications to the ionosphere, *J. Geophys. Res., 66* 1699–1712, 1961.

Hays, P. B., R. A. Jones, and M. H. Rees, Auroral heating and the composition of the neutral atmosphere, *Planet. Space Sci., 21* 559–573, 1973.

Hoegy, W. R., New fine structure cooling rate, *Geophys. Res. Lett., 3,* 541–544, 1976.

Hoffman, J. H., W. H. Dodson, C. R. Lippincott, and H. D. Hammack, Initial ion composition results from the Isis 2 satellite, *J. Geophys. Res., 79,* 4246–4251, 1974.

Jones, R. A., and M. H. Rees, Time dependent studies of the aurora, I, Ion density and composition, *Planet. Space Sci., 21,* 537–557, 1973.

Kofman, W., and V. Wickwar, Plasma line measurements at Chatanika with high-speed correlator and filter bank, *J. Geophys. Res., 85,* 2998–3012, 1980.

Leadabrand, R. L., M. J. Baron, J. Petriceks, and H. F. Bates, Chatanika, Alaska, auroral-zone incoherent-scatter facility, *Radio Sci., 7,* 747–756, 1972.

Moorcroft, D. R., On the determination of temperature and ionic composition by electron backscattering from the ionosphere and magnetosphere, *J. Geophys. Res., 69,* 955–970, 1964.

Newton, G. P., J. C. G. Walker, and G. P. Mantas, Effects of soft electron precipitation on the distribution of vibrational energy of N_2, *J. Geophys. Res., 82* 187–190, 1977.

Oliver, W. L., Models of F_1-region ion composition variations, *J. Atmos. Terr. Phys., 37,* 1065–1076, 1975.

Prasad, S. S., and D. R. Furman, Electron cooling by molecular oxygen, *J. Geophys. Res., 78,* 6701–6707, 1973.

Prölss, G. W., Magnetic storm associated perturbations of the upper atmosphere: Recent results obtained by satellite-borne gas analyzers, *Rev. Geophys. Space Phys., 18,* 183–202, 1980.

Rees, M. H., and J. C. G. Walker, Ion and electron heating by auroral electric fields, *Ann. Geophys., 24,* 193–199, 1968.

Roble, R. G., The thermosphere, in *The Upper Atmosphere and Magnetosphere, Studies in Geophysics,* National Academy of Sciences, Washington, D. C., 1977.

Schlegel, K., and J. P. St. Maurice, Anomalous heating of the polar *E* region by unstable plasma waves, 1, Observations, *J. Geophys. Res.,* in press, 1981.

Schunk, R. W., and P. M. Banks, Auroral N_2 vibrational excitation and the electron density trough, *Geophys. Res. Lett., 2,* 239–242, 1975.

Schunk, R. W., and A. F. Nagy, Electron temperatures in the *F* region of the ionosphere: Theory and observations, *Rev. Geophys. Space Phys., 16,* 355–399, 1978.

Schunk, R. W., W. J. Raitt, and P. M. Banks, Effect of electric fields on the daytime high-latitude *E* and *F* regions, *J. Geophys. Res., 80,* 3121–3130, 1975.

Schunk, R. W., P. M. Banks, and W. J. Raitt, Effects of electric fields and other processes upon the nighttime high-latitude *F* layer, *J. Geophys. Res., 81,* 3271–3282, 1976.

Stubbe, P., and W. S. Varnum, Electron energy transfer rates in the ionosphere, *Planet. Space Sci., 20,* 1121–1126, 1972.

Waldteufel, P., On the analysis of high altitude incoherent scatter data, *Rep. AO 30,* Arecibo Observ., Puerto Rico, 1971.

Walker, J. C. G., and M. H. Rees, Ionospheric electron densities and temperatures in aurora, *Planet. Space Sci., 16,* 459–475, 1968.

Walls, F. L., and G. H. Dunn, Measurement of total cross sections for electron recombination with NO^+ and O_2^+ using ion storage techniques, *J. Geophys. Res., 79,* 1911–1915, 1974.

Wand, R. H., Electron-to-ion temperature ratio from radar Thomson scatter observations, *J. Geophys. Res., 75,* 829–838, 1970.

Wand, R. H., and F. W. Perkins, Temperature and composition of the ionosphere: Diurnal variations and waves, *J. Atmos. Terr. Phys., 32,* 1921–1943, 1970.

Wickwar, V. B., Analysis techniques for incoherent-scatter data interpretation in the 100-to-300 km region, Tech. rep. 3, contract DNA001-72-C-0076, Stanford Res. Inst., Menlo Park, Calif., 1974.

Wickwar, V. B., M. J. Baron, and R. D. Sears, Auroral energy input from energetic electrons and Joule heating at Chatanika, *J. Geophys. Res., 80,* 4364–4367, 1975.

Wickwar, V. B., C. Lathuillere, W. Kofman, and G. Lejeune, Elevated electron temperatures in the auroral *E* layer measured with the Chatanika radar, *J. Geophys. Res., 86,* in press, 1981.

(Received December 17, 1980;
revised April 6, 1981;
accepted April 22, 1981.)